BIOCHEMISTRY
including biophysical chemistry & molecular biology
Article

Biochemistry **2009,** *48,* 11505–11513 11505
DOI: 10.1021/bi901443z

CooC1 from *Carboxydothermus hydrogenoformans* Is a Nickel-Binding ATPase[†]

Jae-Hun Jeoung, Till Giese,[‡] Marlene Grünwald,[§] and Holger Dobbek*

Bioinorganic Chemistry, University of Bayreuth, 95447 Bayreuth, Germany. [‡]*Present address: Lehrstuhl für Biologische Chemie, Technische Universität München, An der Saatzucht 5, D-85350 Freising-Weihenstephan, Germany.* [§]*Present address: Abteilung für Biochemie, Max-Planck-Institut für Entwicklungsbiologie, Spemannstrasse 35, D-72076 Tübingen, Germany.*

Received August 17, 2009; Revised Manuscript Received October 23, 2009

ABSTRACT: The maturation of nickel-dependent enzymes requires the participation of several accessory proteins. Typically the hydrolysis of nucleotides is necessary for the final metal transfer steps. The ATPase CooC has been implicated in the insertion of nickel into the Ni,Fe cluster (C cluster) of the carbon monoxide dehydrogenase from *Rhodospirillum rubrum*. Analysis of the amino acid sequence of CooC suggests the presence of motifs typical for the MinD family of SIMIBI class NTPases, which contain a deviant Walker A motif. The genome of the carboxidotrophic hydrogenogenic bacterium *Carboxydothermus hydrogenoformans* contains three open reading frames with distinct sequence homology to CooC from *R. rubrum*. We overproduced, isolated, and studied CooC1 from *C. hydrogenoformans*. As-isolated CooC1 is monomeric in the absence of ligands but dimerizes in the presence of either nickel, ADP, or ATP. CooC1 shows ATPase activity, and the ADP- and ATP-bound dimeric states are distinguished by their stability. The K8A mutant of CooC1, in which alanine replaces the signature lysine typical for the deviant Walker A motif in the MinD family, is incapable of both ATP hydrolysis and ATP-dependent dimerization. This corroborates that CooC1 is indeed a member of the MinD family and suggests an analogous dynamic equilibrium between monomeric and dimeric states. CooC proteins are involved in the insertion of nickel into carbon monoxide dehydrogenases, and we found that one CooC1 dimer binds one Ni(II) ion with nanomolar affinity. Ni-induced dimerization and the Ni(II)-CooC1 stoichiometry suggest that the Ni-binding site of CooC1 occurs in the dimer interface.

Ni,Fe-dependent CODHases catalyze the reversible oxidation of CO to CO_2 at the active site [$NiFe_4S_4OH_x$] cluster, termed C cluster (*1*−*3*). Possible ways how the C cluster could be assembled have recently been proposed (*4*, *5*), but details on how Ni is delivered to the C cluster are unknown.

The genome of *Rhodospirillum rubrum* contains a five-gene operon (*cooFSCTJ*) encoding the ferredoxin-like protein CooF, CODH (CooS), and three accessory proteins (CooC, CooT, and CooJ), which are involved in Ni insertion (*6*). CooT shows weak sequence similarities to the chaperone-type HypC protein involved in Ni,Fe-hydrogenase maturation (*7*−*9*); however, the function of CooT is unknown (*6*). CooJ contains a COOH-terminal His-rich region similar to UreE and HypB and binds four Ni(II) per monomer with a K_d of 4 μM (*10*). *R. rubrum* cells carrying insertion mutations in the *cooT* and *cooJ* genes show reduced CODH maturation, suggesting that the corresponding proteins are relevant although not essential for Ni insertion into the C cluster (*11*). In the absence of high nickel concentrations the maturation of CODH in *R. rubrum* is dependent on CooC, which has been described as a membrane-associated, homodimeric enzyme with a nucleotide-binding site (P-loop) near the NH_2 terminus necessary for ATPase and GTPase activity (*11*). Homologous expressions of CooC variants unable to hydrolyze ATP and GTP result in the accumulation of inactive, Ni-deficient CODH *in vivo* (*11*).

CooC shows homology to members of the Mrp/MinD family in the SIMIBI class GTPases, which contain a deviant Walker A motif including a highly conserved signature lysine (GKGGhGK[ST], h for any hydrophobic amino acid) (*12*). Members of the Mrp/MinD family are structurally homologous but have diverse cellular functions: MinD works in the spatial regulation of cell division (*13*), Soj assists the plasmid and chromosome segregation (*14*), ArsA acts as an anion pump (*15*), and NifH, in addition to its reductase activity (*16*), inserts Mo/homocitrate into the scaffold protein NifEN in an ATP-dependent manner (*17*). The conformation of Mrp/MinD NTPases is modulated by nucleotide binding; e.g., MinD dimerizes in the presence of ATP (*18*). The dimer of NifH is covalently linked by a [4Fe-4S] cluster, but binding of a transition state analogue induces the formation of a more compact and closed conformation (*19*). Necessary for both processes, ATP-dependent dimerization and conformational compactness, is the presence of the signature lysine, which is indispensable for ATPase activity (*13*).

Carboxydothermus hydrogenoformans is a thermophilic, hydrogenogenic bacterium able to use CO as the sole source of carbon and energy under anaerobic chemolithoautotrophic conditions (*20*). Genome analysis of *C. hydrogenoformans* revealed five open-reading frames encoding CODHases (*21*), of which three CODHases have been studied (*22*, *23*). In addition to the

[†]This work was funded by grants from the Deutsche Forschungsgemeinschaft (DFG, DO-785/1) and supported by the Fonds der chemischen Industrie.

*To whom correspondence should be addressed. Telephone: (++49) 921-554364. Fax: (++49) 921-552432. E-mail: Holger.Dobbek@uni-bayreuth.de.

Published on Web 11/03/2009

Table 1: PCR Primers Used for Cloning and Mutagenesis

Fw_C1[a]	5′-GGA ATT CCA TAT GAA GTT AGC GGT TGC AGG A-3′
Rv_C1[a]	5′-CAT GGT CTC GGA TCC TTA TCC CAC CTC CAA ACG CA-3′
Fw_K8A[b]	5′-GAA GTT AGC GGT TGC AGG A**GC** AGG CGG AGT GGG-3′
Rv_K8A[b]	5′-CCC ACT CCG CCT **GC**T CCT GCA ACC GCT AAC TTC-3′
Fw_C112A[b]	5′-GGT GGA TCC CAA **GC**C TAC TGC CGG GAA AAT TCT T-3′
Rv_C112A[b]	5′-GA ATT TTC CCG GCA GTA G**GC** TTG GGA TCC ACC TT-3′
Fw_C114S[b]	5′-GGT GGA TCC CAA TGC TAC **A**GC CGG GAA AAT TCA-3′
Rv_C114S[b]	5′-GA ATT TTC CCG GC**T** GTA GCA TTG GGA TCC ACC T-3′

[a]Restriction enzyme sites are underlined. [b]Mutations are shown in bold.

CODHases the genome of *C. hydrogenoformans* encodes three isozymes homologous to CooC, termed CooC1, CooC2, and CooC3. The genes encoding CooC1 and CooC2 are part of a genome location responsible for carbon fixation in *C. hydrogenformans* and are positioned close to *cooSIII*, which encodes CODH-III that forms a complex with the acetyl-CoA synthase (*29*). The gene encoding CooC3 is found in a location involved in energy conservation encoding CODH-I and a membrane-bound hydrogenase (*21*). Genes encoding CooT- and CooJ-homologous proteins are not present in the genome of *C. hydrogenoformans* (*21*).

Although it was shown that CooC is important for nickel incorporation into apo-CODH, it could not be demonstrated that CooC binds nickel (*11*). We noticed a conserved motif containing two cysteines (CXC) in CooC proteins, which indicates a potential metal-binding site. Therefore, we investigated the interaction of CooC1 from *C. hydrogenoformans* with nickel and studied its nucleotide-dependent dimerization and ATPase activity.

EXPERIMENTAL PROCEDURES

Chemicals. N_2 and N_2/H_2 (95%/5%) gases were obtained from Riessner-Gase (Lichtenfels, Germany). All restriction enzymes, T4 DNA ligase, and *Pfu* DNA polymerase were obtained from Fermentas. Genes were amplified using the Master Cycler Personal from Eppendorf. All chromatography columns and materials were obtained from GE Healthcare except for the macro-prep ceramic hydroxyapatite (type I, 20 μm) material that was obtained from Bio-Rad. Electrophoresis materials were supplied by Roth. All other chemicals used were at least of analytical grade and obtained from Fluka, Sigma, or Merck. Metal-free water and buffers were prepared by passing over Chelex 100 resin (50−100 mesh, sodium form, Bio-Rad). All anaerobic solutions were prepared in a container (bottle, tube, or cuvette) equipped by screwed cap with butyl rubber or silicon septum either by vigorous sparging of N_2 gas or by successive cycles (at least four cycles) of evacuating and flushing with N_2 gas at a vacuum-gas line.

Cloning, Expression, and Purification. The *cooC1* gene (*21*) was amplified by PCR from the genomic DNA of *C. hydrogenoformans* Z-2901 using *Pfu* DNA polymerase with the primers, Fw_C1 with *Nde*I restriction sites and Rv_C1 with *Eco*31I restriction sites producing a *Bam*HI-compatible ligation site (Table 1). A 791 bp fragment was isolated from 1% (w/v) agarose gel and ligated into a *Nde*I/*Bam*HI-digested pET11a vector (Novagen). Ligation products were transformed into *E. coli* DH5α. A positive plasmid was verified by DNA sequencing (Eurofins MWG Operon, Germany) and named pPKC1. Three primer sets were designed to generate the K8A, C112A, and C114S variants (Table 1) and were used for PCR amplification with the pPKC1 plasmid as a template using the QuickChange method (Stratagene). Plasmids were isolated, and the double point mutations at *aaa* (Lys_8) to *gca* (Ala) for pPKC1K8A and *tgc* (Cys_{112}) to *gcc* (Ala) for pPKC1C112A and a point mutation at *tgc* (Cys_{114}) to *agc* (Ser) for pPKC1C114S plasmids were confirmed by nucleotide sequencing.

Plasmid pPKC1 encoding wild-type CooC1 was transformed into *Escherichia coli* BL21(DE3), which was cultivated in TB medium (*24*) containing carbenicilline under fluxing with compressed air at 37 °C. When OD_{600} reached 0.7−0.8, 0.2 mM IPTG was added to the culture to induce expression of CooC1. The culture was further incubated for 20 h at 37 °C after induction and harvested aerobically. Cell pellet was collected in a glovebox, frozen in liquid N_2, and kept at −30 °C.

The purification was performed under anaerobic conditions inside a glovebox (model B; COY Laboratory Products Inc., MI) under an atmosphere of 95% N_2/5% H_2 at room temperature. Frozen cell paste was resuspended in 100 mL of buffer A (50 mM Tris-HCl, pH 8.0, and 1 mM TCEP)[1] by addition of a small amount of lysozyme and DNase I. After 20 min stirring at room temperature, cells were broken in a glass rosette on ice by sonication (Branson sonifier) under N_2 atmosphere. Cell extracts were further stirred for 30 min at room temperature, followed by centrifugation at 40000 rpm for 1 h to remove cell debris. The supernatant was loaded on a Source 30Q column (30 mL) equilibrated with buffer A, followed by washing the column with the same buffer until the absorption at 280 nm reached zero. Protein was eluted with 300 mL of a linear gradient of 0−1 M NaCl in buffer A. Fractions containing CooC1 protein were pooled, applied to Blue Sepharose fast-flow material (18 mL) equilibrated with buffer A, and eluted with 20 mL of buffer A followed by 200 mL of an increasing linear gradient of 0−1 M NaCl in buffer A. CooC1 was eluted at 150 mM NaCl, combined, and applied to 20 mL of macro-prep ceramic hydroxyapatite equilibrated with buffer B (5 mM $NaH_2PO_4 \cdot 2H_2O$, pH 6.8, and 1 mM TCEP). CooC was eluted at 200 mM phosphate concentration by applying 200 mL of a linear gradient with buffer C (500 mM $NaH_2PO_4 \cdot 2H_2O$, pH 6.8, and 1 mM TCEP). The fractions containing CooC1 were concentrated to 1.5 mL by spin concentrator Vivaspin 70 (10 kDa MWCO; Vivascience GmbH) equipped with a rubber-sealed screw cap. Concentrated CooC1 was loaded on a Superdex 200 prep-grade gel filtration column equilibrated in buffer A containing 300 mM NaCl. The fractions corresponding to monomer size (29 kDa) were collected, and the buffer was exchanged using Sephadex G-25 to metal-free buffer of 20 mM Tris-HCl, pH 8.0, containing 2 mM TCEP. CooC1 was further concentrated, frozen in glass vials equipped with

[1]Abbreviations: TCEP, tris(2-carboxyethyl)phosphine hydrochloride; PAR, 4-(2-pyridylazo)resorcinol; EDTA, ethylenediaminetetraacetic acid.

butyl-rubber septum in liquid N_2, and stored at −70 °C. For productions of the K8A-, C112A-, and C114S-CooC1 variants, a plasmid containing the designated mutation was transformed, cultivated, expressed, and purified as described above for wild-type CooC1.

EDTA Treatment. EDTA-treated CooC1 was generated by incubating as-isolated CooC1 (50 μM dimer) in 10 mM EDTA and 2 mM TCEP solutions for 2 days in an anoxic glovebox at 17 °C. EDTA was removed using a PD10 column (GE Health Care) equilibrated with metal-free buffer of 50 mM Tris-HCl, pH 8.0, and 100 mM NaCl containing 1 mM TCEP (buffer R). Spectra of as-isolated and EDTA-treated apo-CooC1 were obtained on an AnalytikJena SPECORD 40 spectrophotometer with quartz cuvettes (1 cm path length) sealed by silicon septa with screw caps.

Measurements of NTPase Activities. NTPase activities of CooC1 were determined by measuring the amount of inorganic phosphate (P_i) released from hydrolysis of ATP or GTP with a procedure modified from the malachite green assay (*25*). The formation of a phosphomolybdate−malachite green complex was detected by absorbance at 630 nm on an AnalytikJena SPECORD 40 spectrophotometer. Assay solution (400 μL) was prepared in 50 mM Tris-HCl, pH 8.0, containing 100 mM NaCl, 2 mM $MgCl_2$, 2.5 mM ATP or GTP, and 2 mM TCEP. ATP or GTP hydrolysis was initiated by adding CooC1 monomer at a final concentration of 10 μM to the assay solution, and the reaction was allowed to continue for 90 min at room temperature. During the time course of the measurement, aliquots were taken, and absorbance at 630 nm was recorded. To determine the K_m and V_{max} values, ATP concentrations ranging from 0 to 2.5 mM were used, and all kinetics were measured in triplicate for each ATP concentration. Data were fitted to the Michaelis−Menten equation using GraFit 5 (*26*). The amount of P_i released during hydrolysis was calculated from a standard curve prepared by 1−9 nmol of KH_2PO_4. Autohydrolysis of nucleotides in the absence of CooC1 as a control was measured and subtracted from the enzyme-catalyzed reaction. The unit of activity was defined as micromoles of P_i released per minute. The specific activities of enzyme were designated in milliunits per milligram of protein. As dioxygen did not have a significant effect on the NTPase activities, all reactions were performed under aerobic condition except for the ATP hydrolysis of Ni-incubated CooC1 that was measured under anaerobic condition. The concentration of CooC1 was calculated from an extinction coefficient ε_{280} of 19285 M^{-1} cm^{-1} (*27*).

Circular Dichroism (CD) Spectra and Thermal Unfolding Transition. CD measurements were recorded on a JASCO J600 spectropolarimeter with HAAKE K thermostat and a PTC348 W1 Peltier element with N_2 gas flushing. CooC1 was prepared in buffer G (20 mM sodium phosphate, pH 7.5, 100 mM NaCl, and 2 mM TCEP). Final protein concentrations of apo-, Ni-, ATP-, and ADP-CooC1 were 5 and 1 μM monomer in buffer G for far-UV CD spectra and thermal unfolding experiments, respectively. Ten micromolar $NiCl_2$ and 200 μM ATP or ADP were added to generate Ni-CooC1 and ATP- or ADP-CooC1. The standard far-UV CD spectra of the as-isolated, Ni-, ATP-, and ADP-bound CooC1 were collected at 20 °C using a 1 cm path-length cell with a 1 nm bandwidth, 2 s response times, and a scan speed of 20 nm/min. Ten individual scans taken from 190 to 260 nm were added and averaged, followed by subtraction of the solvent CD signal. Thermal denaturation was monitored by measuring the CD signals at 222 nm for as-isolated and Ni-CooC1 and at 225 nm for the ATP- and ADP-CooC1 with increasing temperature from 20 to 80 °C with a temperature scan rate of 60 °C/h. The midpoint of thermal transition (T_m) was calculated by a nonlinear least-squares fit of the experimental data with the heat capacity of 20000 J $mol^{-1}K^{-1}$ (*28*).

Analysis of Oligomeric States of CooC1. Metals were removed from all buffers. Gel filtration experiments were performed at room temperature using a Superdex 200 prep-grade column (16 mm × 600 mm) inside an anaerobic glovebox. Aliquots of wild-type and K8A-CooC1 were dissolved in the running buffer (50 mM Tris-HCl, pH 8.0, 100 mM NaCl, and 2 mM TCEP), injected onto the column equilibrated in the running buffer with or without ligand as noted below, and run with a flow rate of 1 mL/min. Chromatograms were recorded at 280 nm. Approximately 18 μM monomer of as-isolated wild-type CooC1 was subjected to the gel filtration column equilibrated with running buffer with or without 1 mM EDTA. The 36 μM monomer of as-isolated CooC1 was incubated in the running buffer with equimolar concentrations of Ni^{2+} or Zn^{2+} for 10 h at 17 °C in the anoxic glovebox to generate Ni- or Zn-bound CooC1. Binding of Ni was detected by the presence of a peak at 330 nm in the absorption spectrum prior to loading, and the protein was injected in the running buffer containing 2 mM Ni^{2+} or Zn^{2+}. To investigate the nucleotide dependence of the oligomeric states, 36 μM monomer of as-isolated wild-type and 45 μM monomeric K8A-CooC1 were dissolved in the running buffer and loaded on the column equilibrated in the running buffer containing 1 mM ATP or ADP. These experiments were performed two times.

The molecular masses of different states of CooC1 in solution were determined by loading known molecular mass standards in the running buffer: 5 mg/mL catalase (250 kDa), 1 mg/mL aldolase (161 kDa), 1 mg/mL cobalbumin (75 kDa), 1 mg/mL carbonic anhydrase (29 kDa), and 1 mg/mL ribonuclease I (13.7 kDa). A standard curve of molecular weight sieves was generated by plotting elution volume against log MW and fitted to a linear equation (data not shown).

Colorimetric Nickel-Binding Assay. Nickel binding by CooC1 was detected by a colorimetric method using a PAR solution as described (*29*). Protein samples were diluted to 50 μM dimer in buffer A. To determine the stoichiometry of Ni^{2+} bound to CooC1, different molar ratios of nickel to CooC1 (1:1, 2:1, and 4:1) were added to the protein solution and incubated for 1 h under anaerobic conditions. Unbound nickel was removed by cycles of concentration and dilution with buffer A until the theoretical free nickel concentration in solution was less than 1 μM. Nickel was released by incubating Ni-treated CooC1 for 3 min with 4 M guanidine hydrochloride. The amount of nickel released by unfolding was measured by absorption at 500 nm with 100 μM PAR solution and quantified using a standard curve produced with different nickel concentrations in the presence of PAR measured under the same conditions as in the protein assay.

UV−Visible Spectroscopy and Nickel Titration. As-isolated CooC1 (apoprotein) was used for all measurements. Metal-free water and buffers were used throughout this study. The salt concentration in the assay buffer was adjusted to 100 mM NaCl in 50 mM Tris-HCl, pH 8.0 (buffer T). A total of 1 mL reaction solution was prepared inside the anoxic glovebox by dissolving 32−36 μM CooC1 (monomeric) of the wild-type or K8A-CooC1 in buffer T with or without 100 μM ATP or ADP supplemented with 1 mM TCEP. Nickel was added in steps of 1−5 μL with a gastight syringe (Hamilton) from a 1 mM $NiCl_2$ solution

prepared anaerobically. After each addition time was given to allow for equilibration of the solution, and absorption spectra were recorded from 250 to 500 nm and corrected against buffer with equivalent nickel concentrations. Each spectrum was recorded within 5 min. All spectra were corrected for dilution. Titration data were fitted to the following equation (eq 1) using GraFit 5 (*26*):

$$\delta A_{(330\text{nm})} = \frac{\delta A_{\max(330\text{nm})}}{2nE_T}\left[(L_T + nE_T + K_d) - \sqrt{(L_T + nE_T + K_d)^2 - (4L_T nE_T)}\right] \quad (1)$$

where $\delta A_{(330\text{nm})}$ and $\delta A_{\max(330\text{nm})}$ are the actual and maximal absorption difference at 330 nm, respectively, n is the number of nickel-binding sites at dimeric CooC1, E_T and L_T are the total concentrations of CooC1 dimer and Ni^{2+}, respectively, and K_d is the dissociation constant.

RESULTS

Characterization of CooC1. CooC1 from *C. hydrogenoformans* was expressed in *E. coli*, and the protein was purified under anaerobic conditions. Four chromatography steps were sufficient to produce pure and homogeneous CooC1, as evidenced by a band at approximately 28 kDa in reducing SDS−PAGE (see Supporting Information Figure S1). As-isolated CooC1 and EDTA-treated CooC1 proteins show practically identical features in UV−vis absorption spectra and behaved identically in the analytical gel filtration and nickel titration. Therefore, as-isolated CooC1 is equivalent to EDTA-treated protein, respectively apo-CooC1. As-isolated CooC1 showed a specific ATPase activity of 5.1 ± 0.6 nmol min^{-1} (mg of protein)$^{-1}$ but no detectable GTPase activity (Figure 1). The ATPase activity of CooC1 was strictly dependent on the presence of Mg^{2+} in the assay. When CooC1 was incubated with Ni^{2+}, the specific activity in ATP hydrolysis decreased marginally to 4.4 ± 0.3 nmol min^{-1} (mg of protein)$^{-1}$ (Figure 1). A CooC1 variant in which Lys_8 (8-**K**GGVGGKT-15) was replaced by alanine was generated, expressed, and purified as wild type. K8A-CooC1 exhibits no ATPase activity (Figure 1A), indicating that the signature lysine (Lys_8) is essential for ATP hydrolysis.

To determine the Michaelis−Menten parameters of the ATPase activity of CooC1, its activity was measured at varying ATP concentrations. The dependence of the activity upon ATP concentration shows clear saturation behavior (Figure 1B). By fitting the data against the Michaelis−Menten equation using nonlinear regression analysis, the K_m and V_{max} for ATP hydrolysis of CooC1 were determined as 44.3 ± 7.4 μM and 5.0 ± 0.2 nmol min^{-1} (mg of protein)$^{-1}$, respectively.

The far-UV CD spectra of CooC1 exhibited the characteristic features of an α-helical protein, identified from two minima at 208 and 222 nm (data not shown). The far-UV CD spectra of CooC1 showed little perturbation in the presence of nickel, ATP, or ADP, indicating a minimal net change in secondary structure due to ligand binding. CooC1 is a protein from a thermophilic organism, and we were therefore interested in its resistance against thermally induced unfolding. As-isolated apo-CooC1 showed a midpoint thermal transition (T_m) of 66.4 °C (Figure 2) and binding of Ni or ATP increased the T_m by approximately 1 °C while binding of ADP decreased the T_m by 1 °C compared to apo-CooC1. The results suggest that the binding of these ligands

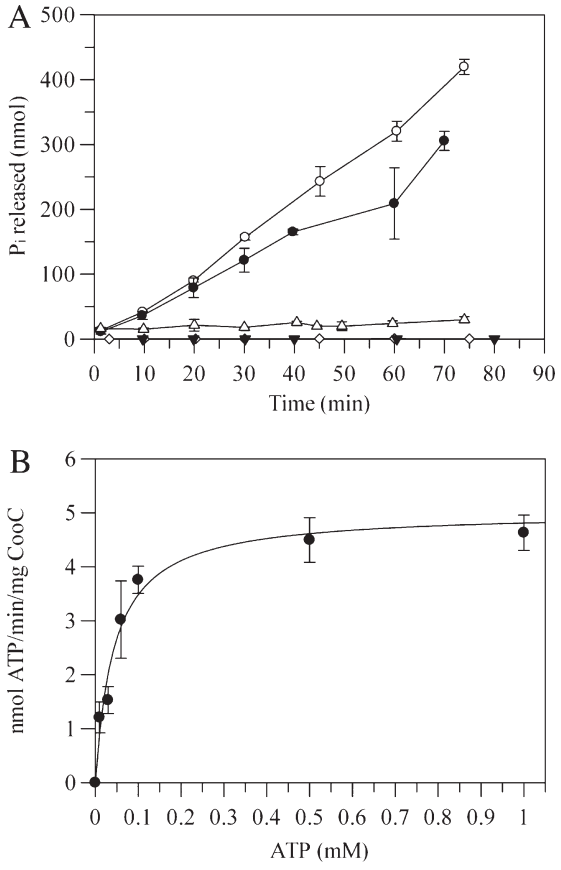

FIGURE 1: NTPase activities of CooC1. (A) ATP and GTP hydrolysis of wild type (○ and △, respectively) and ATP hydrolysis of Ni-incubated wild type (●) and K8A-CooC1 (▼) in the presence of $MgCl_2$. Given amounts of P_i values were corrected for the autohydrolysis of the nucleotides (◇). Assay solutions contained 100 mM NaCl, 2 mM $MgCl_2$, 2.5 mM ATP or GTP, and 2 mM TCEP in 50 mM Tris-HCl, pH 8.0, and reactions were initiated by adding CooC1 as final concentration of 10 μM monomer into the assay solution at room temperature. The error bars were calculated from at least three independent measurements. (B) Dependence of the ATP hydrolysis rate on ATP concentration. At each substrate concentration, hydrolysis of ATP was measured in triplicate. Analysis of the data revealed a K_m value of 44.3 ± 7.4 μM and a V_{max} of 5.0 ± 0.2 nmol min^{-1} (mg of protein)$^{-1}$.

neither changes the fold nor does it significantly influence the thermal stability of CooC1.

UV−visible spectra of as-isolated CooC1 showed only a characteristic peak at 280 nm (Figure 3A). Spectral features characteristic for metal-bound states, as, for example, Fe-S clusters, were not observed.

Stoichiometric Binding of Nickel by CooC1. We analyzed the ability of CooC1 to bind nickel using UV−visible spectroscopy and a colorimetric nickel-binding assay. The colorimetric assay was used to determine if CooC1 binds Ni^{2+} ions and, if so, to analyze the stoichiometry between protein and metal ion. Following repeated cycles of concentrating and diluting Ni-incubated CooC1 to remove unbound Ni^{2+} ions, we used PAR to detect the amount of Ni^{2+} liberated after unfolding CooC1 (Table 2). A ratio of approximately one Ni^{2+} ion per dimer of CooC1 was determined independent of the Ni^{2+} concentration used to incubate CooC1. The amount of nickel bound to CooC1 detected in the assay is slightly decreasing with higher Ni^{2+} concentrations (Table 2). This at first glance counterintuitive observation most likely reflects the limits of the experimental procedure. As Ni binds reversibly to CooC1, it is slowly lost

during the dilution and concentration steps. A larger number of cycles of dilution and concentration of Ni-incubated CooC1 are necessary to bring the theoretical concentration of free Ni^{2+} below 1 μM when higher concentrations of Ni^{2+} are used.

To determine whether the interaction of CooC1 with Ni^{2+} changes the UV/vis spectrum of the protein, we measured the spectrum of as-isolated CooC1 before and after the addition of $NiCl_2$. The addition of 1 equiv of $NiCl_2$ to 2 equiv of CooC1 under anoxic reducing conditions produced a distinct broad peak with a maximum at 330 nm (ε_{330} = 4.7 × 10^3 M^{-1} cm^{-1}). To verify the stoichiometry found in the colorimetric assay and determine the affinity of the interaction between Ni(II) and CooC1, we titrated the protein by a stepwise addition from a $NiCl_2$ stock solution and recorded spectra after each step (Figure 4). Maxima at 280 and 330 nm are clearly visible in difference spectra of the titration (Figure 4A). Intensity and position of the two peaks suggest that they originate from a ligand-to-metal charge transfer (LMCT) between Cys-S_γ^- and Ni(II) (*30*, *31*). The absorbance change shows a clear saturation behavior with increasing Ni(II) concentrations, and nonlinear regression analysis using eq 1 (Figure 4B) indicates the binding of 0.93 ± 0.01 mol of Ni(II) per dimer of CooC1 with a K_d of 0.41 ± 0.05 μM.

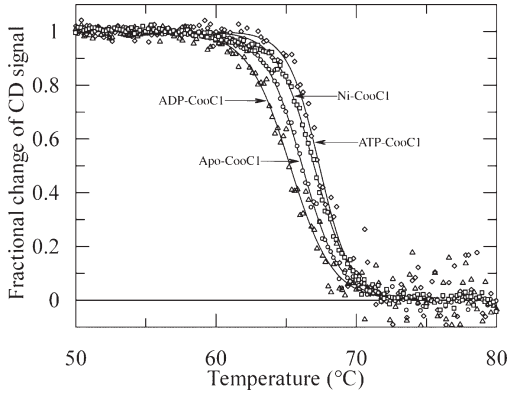

FIGURE 2: Thermal denaturation profile of CooC1. The transitions of 1 μM apo-CooC1 monomer in 20 mM sodium phosphate, pH 7.5, 100 mM NaCl, and 2 mM TCEP in the absence (○) and the presence of 10 μM $NiCl_2$ (□), 200 μM ATP (◇), or 200 μM ADP (△) were measured by CD spectroscopy at 222 nm for apo- and Ni-CooC1 and at 225 nm for ATP- and ADP-CooC1 over a linear temperature gradient from 20 to 80 °C at 60 °C/h. Values of midpoint thermal transition for apo-, Ni-, ATP-, and ADP-CooC1 were calculated as 66.4, 67.5, 67.1, and 65.4 °C, respectively.

To verify the involvement of Cys residues in Ni(II) binding, two highly conserved cysteines were mutated either to Ala (C112A variant) or to Ser (C114S variant) and were purified like wild-type CooC1. While the spectral features of the as-isolated states of both variants are identical to that of the wild-type protein, the spectra of the C112A and C114S variants did not change upon addition and incubation with equivalent amounts of Ni(II), unlike the wild-type protein.

The K8A-CooC1 variant showed the same spectral features as the wild type after incubation with Ni(II) (ε_{330} = 4.5 × 10^3 M^{-1} cm^{-1}), indicating that Lys_8, although essential for ATP hydrolysis, does not influence the nickel- binding site of CooC1. However, the spectrum was shifted to longer wavelength and reveals a split of the observed maxima at 286, 295, and 341 nm and a shoulder around 380 nm when CooC1 was incubated with 100 μM ATP or ADP before Ni(II) was added (Figure 3B). The observed difference spectra of the CooC1−Ni complex were the same in the presence of ADP and ATP. Additionally, a shoulder with small extinction coefficient (< 400 M^{-1} cm^{-1}) at 620 nm developed in the presence of both nucleotides, which has not been observed with Ni-incubated CooC1 alone. These results suggest that the binding of ATP and ADP alters the conformation of the nickel-binding site of CooC1.

Metal- and Nucleotide-Dependent Dimerization of CooC1. The native molecular mass of as-isolated CooC1 was estimated to be 32 kDa by analytical gel filtration, corresponding to a monomeric state in solution (Figure 5A). Size-exclusion chromatography was also used to test whether CooC1 forms a dimer in the presence of 2 mM $NiCl_2$ in the running buffer (Figure 5A). Chromatograms of CooC1 with $NiCl_2$ revealed the presence of two populations corresponding to monomeric

Table 2: Colorimetric Detection of Stoichiometric Nickel Binding by CooC1[a]

concn of Ni^{2+} added (μM)	detection of Ni^{2+} with PAR (μM)	molar ratio of Ni^{2+} to CooC1 dimer
0[b]	n/d[c]	
50	42.8 ± 2.7	1.08 ± 0.07
100	38.9 ± 5.8	0.96 ± 0.21
200	35.9 ± 4.2	0.82 ± 0.05

[a]Final protein concentration was 50 μM CooC1 dimer. [b]Apo-CooC1. [c]Not detected.

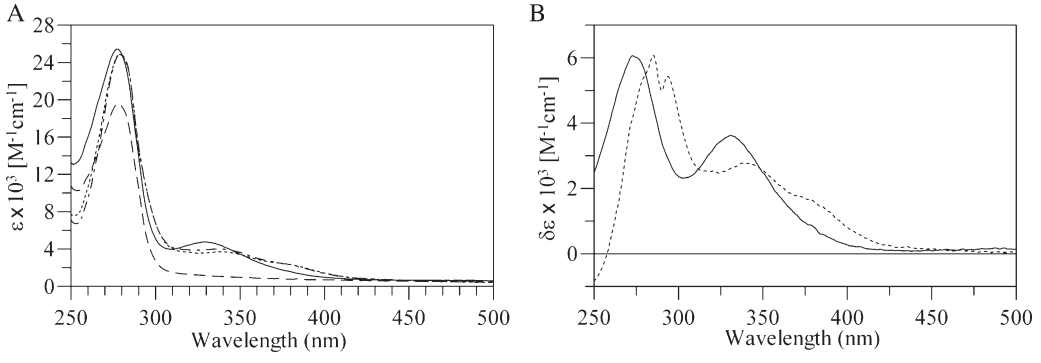

FIGURE 3: UV−visible spectra of CooC1. (A) A spectrum of apo-CooC1 (34 μM monomer) in 50 mM Tris-HCl, pH 8.0, 100 mM NaCl, and 1 mM TCEP was recorded (dashed line). Addition of 0.5 nickel equivalent resulted in a broad peak with a maximum at 330 nm (solid line), with an ε_{330} of (4.7 ± 0.1) × 10^3 M^{-1} cm^{-1}. Addition of 0.5 nickel equivalent in the presence of 100 μM ATP or ADP gives absorption maxima at longer wavelength (dotted and dashed-dotted lines, respectively), which are discernible in difference spectra (B) with maxima at 286, 295, and 341 nm and a shoulder around 380 nm.

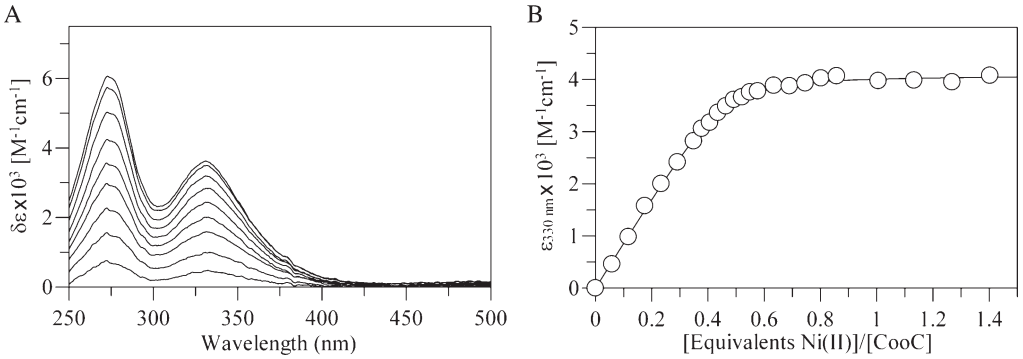

FIGURE 4: Nickel titration of CooC1. (A) Difference spectrum of CooC1 with increasing amounts of Ni minus apo-CooC1 (as in Figure 3A). (B) Extinction difference at 330 nm plotted against nickel concentration. Nonlinear regression analysis of the titration data using eq 1 gives a stoichiometry of 0.93 ± 0.01 mol of Ni(II) per dimeric CooC1 and a K_d of 0.41 ± 0.05 μM.

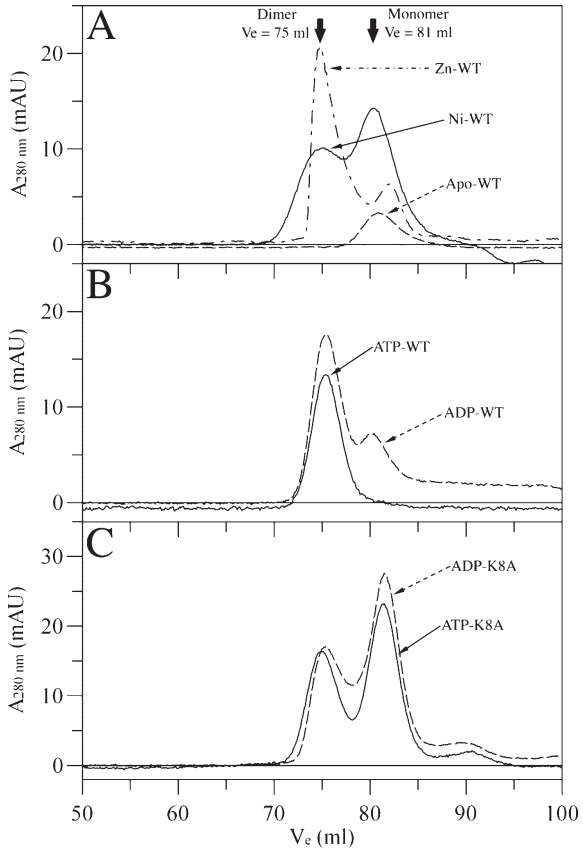

FIGURE 5: Analysis of metal- and nucleotide-dependent dimerization of CooC1 by gel filtration chromatography. Approximately 2 and 3 mg of wild-type and K8A-CooC1 were injected onto a Superdex 200 prep-grade column in a metal-free running buffer (50 mM Tris-HCl, pH 8.0, 100 mM NaCl, and 2 mM TCEP) with or without effectors and run with a flow rate of 1 mL/min. Elution profiles were recorded by following the absorption at 280 nm. (A) Elution profiles of wild-type apo-CooC1 (dashed line) and apo-CooC1 treated with 2 mM $NiCl_2$ (solid line) and 2 mM $ZnCl_2$ (dash-dotted line) prior to run for 10 h at 17 °C are shown. Metal-incubated CooC1 samples were chromatographed in the presence of either 2 mM $NiCl_2$ or 2 mM $ZnCl_2$. (B) Wild-type and (C) K8A-CooC1 incubated in running buffer with nucleotides were loaded on the column equilibrated in the presence of 1 mM ATP (solid line) or ADP (dashed line). All experiments were performed twice. Elution volumes (V_e) of monomer and dimer are indicated and correspond to 32 and 54 kDa, respectively.

(32 kDa) and dimeric CooC1 (54 kDa), implying that nickel binding induces dimerization of CooC1. The same behavior of CooC1 was observed in the presence of $ZnCl_2$ (Figure 5A), which indicates that CooC1 possesses a metal-binding site at the dimer interface for both Ni(II) and Zn(II). Wild-type CooC1 showed peaks at 35 and 53 kDa in the presence of ADP corresponding to a mixture of monomeric and dimeric CooC1 (Figure 5B). However, in the presence of ATP only one symmetric peak is observed corresponding to dimeric CooC1 (53 kDa), suggesting the protein forms a stable dimeric state upon binding to ATP (Figure 5B). The exchange of lysine 8 against alanine in CooC1 (K8A-CooC1) increases the ratio of monomeric CooC1 regardless of the nucleotide present (Figure 5C).

DISCUSSION

The binding and hydrolysis of nucleotides are prerequisites for CooC proteins and homologous NTPases to support diverse biological functions. To investigate how ADP and ATP influence the properties of CooC1 from *C. hydrogenoformans*, we investigated the ATPase activity, monomer−dimer equilibrium, and nickel-binding properties of the enzyme, which we can now compare to related proteins. A dynamic equilibrium between monomeric and dimeric states is a distinct property of many MinD-type ATPases (*13*). As-isolated CooC1 is a monomer in solution and dimerizes in the presence of nickel and ADP and ATP. For as-isolated CooC from *R. rubrum* a homodimeric state with 61−63 kDa was reported (*11*). CooC from *R. rubrum* is an ATPase and showed low GTPase activity, while CooC1 has only ATPase activity, which is 15-fold lower than that of CooC from *R. rubrum*. This difference may partly be due to the difference in assay temperatures, which was 37 °C in case of *R. rubrum* CooC, while we carried out our assays at room temperature. However, the most important difference is probably that CooC1 is an ATPase of a thermophilic organism with an optimal growth temperature of 78 °C (*20*), while *R. rubrum* is a mesophilic organism.

The primary sequence alignment of CooC proteins with members of the Mrp/MinD family shows conserved motifs for nucleotide hydrolysis, specifically a deviant Walker A motif with two essential lysine residues (G**K**GGhG**K**[ST]) (*12*, *32*), namely, the canonical P-loop lysine in the C-terminal part of the motif and the signature lysine in the synapomorphic, N-terminal KGG signature (Figure 6). That the canonical P-loop lysine is required by CooC has already been demonstrated for CooC from *R. rubrum* (*11*). The exchange of the signature lysine to alanine in the K8A-CooC1 variant completely abolished the ATPase activity, suggesting a role for the signature lysine in CooC similar to that of other MinD-type ATPases. The signature lysine of CooC1 not

FIGURE 6: Conserved deviant Walker A (P-loop) and CXC motifs of CooC homologues. The signature lysine in the synapomorphic KGG signature of the deviant Walker A motif is marked by an asterisk, and the conserved cysteines (Cys_{112} and Cys_{114} in CooC1_Ch) in the CXC motif are indicated by arrows. Sequence identities of CooC1_Ch to others are 26% to CooC2_Ch, 41% to CooC3_Ch, 34% to CooC_Rr, 21% to AcsF_Mt, 17% to MinD_Pf, and 16% to Soj_Tt. Abbreviations: Ch, *C. hydrogenoformans*; Rr, *R. rubrum*; Mt, *Moorella thermoacetica*; Pf, *Pyrococcus furiosus*; Tt, *Thermus thermophilus*. Amino acid sequences were aligned with ClustalW2 (50): 100%, 80%, and 70% conserved residues are blocked in black, dark gray, and light gray, respectively, and shown only in partial.

only is necessary for ATPase activity but also contributes in stabilizing the dimeric states with ADP and ATP. The crystal structures of MinD from *E. coli* (*18*) and NifH from *Azotobacter vinelandii* (*19*) demonstrate that the signature lysine contributes to a compact dimeric state by interacting across the dimer interface with the terminal oxygen atom of the β-phosphate group of ATP in the second monomer. Other homologues, such as AcsF from *Clostridium thermoaceticum* (*33*), NifH of *A. vinelandii* (*34*), and HypB of *E. coli* and *Bradyrhizobium japonicum* (*35*), hydrolyze either only GTP or ATP. The observed low ATPase activity of CooC1 is similar to what is observed for HypB (*36*), MinD (*13*), Soj (*14*), and NifH (*19*), which typically show increased activities after binding to a partner protein. A stimulation of the ATPase activity of CooC1 in the presence of nickel was not observed, and the partner protein of CooC1 is currently unknown.

We demonstrated that CooC1 is a nickel-binding ATPase with a stoichiometry of one nickel ion per dimer. The involvement of cysteine residues in the binding of nickel is indicated by the characteristic signal of a Cys-S_γ^- to Ni(II) LMCT in the UV/vis spectrum (Figure 3). We observed two cysteine residues within a CXC motif, which is highly conserved for proteins homologous to CooC and is absent in other MinD-type ATPases (Figure 6). The involvement of the two cysteine residues of the CXC motif of CooC1 in Ni binding is further confirmed through the inability of CooC1 to bind Ni(II) when one of the cysteines is exchanged against another residue (C112A and C114S). The spectroscopic signature of the CooC1−nickel complex and its stoichiometry show that CooC1 binds nickel, which has not been observed for CooC from *R. rubrum* (*11*). We showed that the presence of ATP or ADP modulates the spectral characteristics of the Ni-bound CooC1 complex (Figure 3). In the presence of ADP or ATP bands at longer wavelength are observed that are assignable to LMCTs from Cys-S_γ^- or His-N to Ni(II) and a band at the lower energies (620 nm) with small extinction coefficient indicative of a d−d transition of Ni(II), suggesting changes in the coordination of Ni(II) upon ATP/ADP binding (*30*, *37*−*39*). This is evidence for a functional coupling between the nucleotide and the metal-binding sites.

Cells show elaborate mechanisms to scavenge, store, and transport metals ions needed in a variety of physiological processes (*40*). Nickel is an essential component of metalloenzymes such as hydrogenases, ureases, and Ni,Fe-containing carbon monoxide dehydrogenases (CODHases) (*41*). The biosynthesis of nickel-containing enzymes requires the participation of several accessory proteins, and independent pathways have been proposed for each type of enzyme (*42*). However, insertion of nickel into the precursor enzyme involves two common processes: nickel binding and nucleotide hydrolysis (*42*). Urease matures when a Ni ion is delivered to the complex of apo-urease and UreDFG by the metallochaperone UreE (*43*). Part of the UreDFG complex is the GTPase UreG, which is necessary for nickel incorporation into apo-urease (*44*). The assembly of Ni−Fe hydrogenases is even more complex than that of urease and additionally involves proteolytic processing and the biosynthesis and attachment of the small molecular ligands CN^- and CO (*42*). However, incorporation of nickel into apo-hydrogenase is also a GTP-dependent reaction requiring the nickel-binding GTPase HypB (*45*, *46*). The crystal structure of HypB from *Methanocaldococcus jannaschii* revealed two metal-binding sites per HypB monomer, one of which is dependent on the binding of nucleotide in the dimer interface and coordinates metals with conserved cysteine and histidine residues (*36*). *E. coli* HypB possesses a conserved NH_2-terminal CXXCGC motif that is absent in archaeal HypB proteins, which binds one equivalent of Ni(II) with a dissociation constant in the subpicomolar range (*46*), and both metal-binding sites are functionally relevant and influence each other (*47*).

Dimer formation of CooC1 appears essential for two processes: the hydrolysis of ATP and the binding of nickel. Conversely, binding of ATP/ADP and nickel induces dimerization of CooC1. Nucleotide-dependent dimerization occurs more completely with ATP than with ADP (Figure 5B) and is stabilized by the signature lysine, whose mutation to alanine shifts the monomer−dimer equilibrium to the monomeric state (Figure 5C). This agrees with a conserved role for the signature lysine in the MinD family in driving an ATP-dependent dimerization before hydrolysis can occur. Like CooC, HypB and NifH are involved in the NTP-dependent assembly of enzymatic metal centers (*46*, *17*). All three proteins belong to the SIMIBI class of NTPases. Strikingly, a binding partner of NifH, the nitrogenase MoFe protein, and the likely partner of CooC, the Ni,Fe-containing CODHase, share common structural motifs especially around their active site metal clusters (*48*), making it tempting to speculate on conserved modes of recognition and interaction in the resulting protein complexes. Metal-induced dimerization has recently been reported for UreG from *Helicobacter pylorii* (*49*). The binding of one Zn^{2+} ion induces two UreG monomers to dimerize, and the authors suggested the dimeric state to be the active form. Further work is necessary to establish the role of the CooC-bound Ni ion and its connection to the insertion of nickel into CODHases.

ACKNOWLEDGMENT

Dr. Roman Jakob (Biochemistry, University of Bayreuth) is acknowledged for recording and evaluating the CD spectra.

SUPPORTING INFORMATION AVAILABLE

One figure showing Coomassie blue-stained 12% (w/v) SDS−PAGE of the overproduction and chromatographic purification of CooC1. This material is available free of charge via the Internet at http://pubs.acs.org.

REFERENCES

1. Dobbek, H., Svetlitchnyi, V., Gremer, L., Huber, R., and Meyer, O. (2001) Crystal structure of a carbon monoxide dehydrogenase reveals a [Ni-4Fe-5S] cluster. *Science 293*, 1281–1285.
2. Drennan, C. L., Heo, J. Y., Sintchak, M. D., Schreiter, E., and Ludden, P. W. (2001) Life on carbon monoxide: X-ray structure of *Rhodospirillum rubrum* Ni-Fe-S carbon monoxide dehydrogenase. *Proc. Natl. Acad. Sci. U.S.A. 98*, 11973–11978.
3. Darnault, C., Volbeda, A., Kim, E. J., Legrand, P., Vernede, X., Lindahl, P. A., and Fontecilla-Camps, J. C. (2003) Ni-Zn-[Fe4-S4] and Ni-Ni-[Fe4-S4] clusters in closed and open subunits of acetyl-CoA synthase/carbon monoxide dehydrogenase. *Nat. Struct. Biol. 10*, 271–279.
4. Lindahl, P. A., and Graham, D. E. (2007) Acetyl-coenzyme A synthases and nickel-containing carbon monoxide dehydrogenases. *Met. Ions Life Sci. 2*, 357–416.
5. Jeon, W. B., Singer, S. W., Ludden, P. W., and Rubio, L. M. (2005) New insights into the mechanism of nickel insertion into carbon monoxide dehydrogenase: analysis of *Rhodospirillum rubrum* carbon monoxide dehydrogenase variants with substituted ligands to the [Fe3S4] portion of the active-site C-cluster. *J. Biol. Inorg. Chem. 10*, 903–912.
6. Kerby, R. L., Ludden, P. W., and Roberts, G. P. (1997) *In vivo* nickel insertion into the carbon monoxide dehydrogenase of *Rhodospirillum rubrum*: molecular and physiological characterization of *cooCTJ*. *J. Bacteriol. 179*, 2259–2266.
7. Blokesch, M., and Bock, A. (2002) Maturation of [NiFe]-hydrogenases in *Escherichia coli*: The HypC cycle. *J. Mol. Biol. 324*, 287–296.
8. Blokesch, M., Albracht, S. P. J., Matzanke, B. F., Drapal, N. M., Jacobi, A., and Bock, A. (2004) The complex between hydrogenase-maturation proteins HypC and HypD is an intermediate in the supply of cyanide to the active site iron of [NiFe]-hydrogenases. *J. Mol. Biol. 344*, 155–167.
9. Watanabe, S., Matsumi, R., Arai, T., Atomi, H., Imanaka, T., and Miki, K. (2007) Crystal structures of [NiFe] hydrogenase maturation proteins HypC, HypD, and HypE: insights into cyanation reaction by thiol redox signaling. *Mol. Cell 27*, 29–40.
10. Watt, R. K., and Ludden, P. W. (1998) The identification, purification, and characterization of CooJ—a nickel-binding protein that is CO-regulated with the Ni-containing CO dehydrogenase from *Rhodospirillum rubrum*. *J. Biol. Chem. 273*, 10019–10025.
11. Jeon, W. B., Cheng, J. J., and Ludden, P. W. (2001) Purification and characterization of membrane-associated CooC protein and its functional role in the insertion of nickel into carbon monoxide dehydrogenase from *Rhodospirillum rubrum*. *J. Biol. Chem. 276*, 38602–38609.
12. Leipe, D. D., Wolf, Y. I., Koonin, E. V., and Aravind, L. (2002) Classification and evolution of P-loop GTPases and related ATPases. *J. Mol. Biol. 317*, 41–72.
13. Lutkenhaus, J., and Sundaramoorthy, M. (2003) MinD and role of the deviant Walker A motif, dimerization and membrane binding in oscillation. *Mol. Microbiol. 48*, 295–303.
14. Leonard, T. A., Butler, P. J., and Lowe, J. (2005) Bacterial chromosome segregation: structure and DNA binding of the Soj dimer—a conserved biological switch. *EMBO J. 24*, 270–282.
15. Zhou, T. Q., Radaev, S., Rosen, B. P., and Gatti, D. L. (2000) Structure of the ArsA ATPase: the catalytic subunit of a heavy metal resistance pump. *EMBO J. 19*, 4838–4845.
16. Hageman, R. V., and Burris, R. H. (1978) Nitrogenase and nitrogenase reductase associate and dissociate with each catalytic cycle. *Proc. Natl. Acad. Sci. U.S.A. 75*, 2699–2702.
17. Hu, Y. L., Corbett, M. C., Fay, A. W., Webber, J. A., Hodgson, K. O., Hedman, B., and Ribbe, M. W. (2006) FeMo cofactor maturation on NifEN. *Proc. Natl. Acad. Sci. U.S.A. 103*, 17119–17124.
18. Hayashi, I., Oyama, T., and Morikawa, K. (2001) Structural and functional studies of MinD ATPase: implications for the molecular recognition of the bacterial cell division apparatus. *EMBO J. 20*, 1819–1828.
19. Schindelin, N., Kisker, C., Sehlessman, J. L., Howard, J. B., and Rees, D. C. (1997) Structure of ADP·AlF_4-stabilized nitrogenase complex and its implications for signal transduction. *Nature 387*, 370–376.
20. Svetlichny, V. A., Sokolova, T. G., Gerhardt, M., Ringpfeil, M., Kostrikina, N. A., and Zavarzin, G. A. (1991) *Carboxydothermus hydrogenoformans* Gen-Nov, Sp-Nov, a co-utilizing thermophilic anaerobic bacterium from hydrothermal environments of Kunashir Island. *Syst. Appl. Microbiol. 14*, 254–260.
21. Wu, M., Ren, Q. H., Durkin, A. S., Daugherty, S. C., Brinkac, L. M., Dodson, R. J., Madupu, R., Sullivan, S. A., Kolonay, J. F., Nelson, W. C., Tallon, L. J., Jones, K. M., Ulrich, L. E., Gonzalez, J. M., Zhulin, I. B., Robb, F. T., and Eisen, J. A. (2005) Life in hot carbon monoxide: the complete genome sequence of *Carboxydothermus hydrogenoformans* Z-2901. *PLoS Genet. 1*, 563–574.
22. Svetlitchnyi, V., Dobbek, H., Meyer-Klaucke, W., Meins, T., Thiele, B., Romer, P., Huber, R., and Meyer, O. (2004) A functional Ni-Ni-[4Fe-4S] cluster in the monomeric acetyl-CoA synthase from *Carboxydothermus hydrogenoformans*. *Proc. Natl. Acad. Sci. U.S.A. 101*, 446–451.
23. Svetlitchnyi, V., Peschel, C., Acker, G., and Meyer, O. (2001) Two membrane-associated NiFeS-carbon monoxide dehydrogenases from the anaerobic carbon-monoxide-utilizing eubacterium *Carboxydothermus hydrogenoformans*. *J. Bacteriol. 183*, 5134–5144.
24. Sambrook, J., Fritsch, E. F., and Maniatis, T. (1989) Molecular Cloning: A Laboratory Manual , 2nd ed., Cold Spring Harbor Laboratory, Cold Spring Harbor, NY.
25. Lanzetta, P. A., Alvarez, L. J., Reinach, P. S., and Candia, O. A. (1979) Improved assay for nanomole amounts of inorganic-phosphate. *Anal. Biochem. 100*, 95–97.
26. Leatherbarrow, R. J. (2001) GraFit Version 5, Ltd., E. S., ed., Horley, U.K.
27. Pace, C. N., Vajdos, F., Fee, L., Grimsley, G., and Gray, T. (1995) How to measure and predict the molar absorption coefficient of a protein. *Protein Sci. 4*, 2411–2423.
28. Mayr, L. M., Landt, O., Hahn, U., and Schmid, F. X. (1993) Stability and folding kinetics of ribonuclease-T(1) are strongly altered by the replacement of cis-proline-39 with alanine. *J. Mol. Biol. 231*, 897–912.
29. Jezorek, J. R., and Freiser, H. (1979) 4-(Pyridylazo)resorcinol-based continuous detection system for trace levels of metal-ions. *Anal. Chem. 51*, 373–376.
30. Kozlowski, H., Decocklereverend, B., Ficheux, D., Loucheux, C., and Sovago, I. (1987) Nickel(II) complexes with sulfhydryl containing peptides—potentiometric and spectroscopic studies. *J. Inorg. Biochem. 29*, 187–197.
31. Jeffrey, S., Iwig, S. L., Herbst, R. W., Maroney, M. J., and Chivers, P. T. (2008) Ni(II) and Co(II) sensing by *Escherichia coli* RcnR. *J. Am. Chem. Soc. 130*, 7592–7606.
32. Koonin, E. V. (1993) A superfamily of ATPases with diverse functions containing either classical or deviant ATP-binding motif. *J. Mol. Biol. 232*, 1013–1013.
33. Loke, H. K., and Lindahl, P. A. (2003) Identification and preliminary characterization of AcsF, a putative Ni-insertase used in the biosynthesis of acetyl-CoA synthase from *Clostridium thermoaceticum*. *J. Inorg. Biochem. 93*, 33–40.
34. Ryle, M. J., and Seefeldt, L. C. (2000) Hydrolysis of nucleoside triphosphates other than ATP by nitrogenase. *J. Biol. Chem. 275*, 6214–6219.
35. Fu, C. L., Olson, J. W., and Maier, R. J. (1995) HypB protein of *Bradyrhizobium japonicum* is a metal-binding GTPase capable of binding 18 divalent nickel ions per dimer. *Proc. Natl. Acad. Sci. U.S.A. 92*, 2333–2337.
36. Gasper, R., Scrima, A., and Wittinghofer, A. (2006) Structural insights into HypB, a GTP-binding protein that regulates metal binding. *J. Biol. Chem. 281*, 27492–27502.
37. Pereira, E., Gomes, L., and de Castro, B. (1998) Synthesis, spectroscopic and electrochemical study of nickel(II) complexes with tetradentate asymmetric Schiff bases derived from salicylaldehyde and methyl-2-amino-1-cyclopentenedithiocarboxylate. *Inorg. Chim. Acta 271*, 83–92.
38. Ge, R., Watt, R. M., Sun, X., Tanner, J. A., He, Q.-Y., Huang, J.-D., and Sun, H. (2006) Expression and characterization of a histidine-rich protein, Hpn: potential for Ni^{2+} storage in *Helicobacter pylori*. *Biochem. J. 393*, 285–293.
39. Cavet, J. S., Graham, A. I., Meng, W. M., and Robinson, N. J. (2003) A cadmium-lead-sensing ArsR-SmtB repressor with novel sensory sites—complementary metal discrimination by NMTR and CMTR in a common cytosol. *J. Biol. Chem. 278*, 44560–44566.
40. Waldron, K. J., and Robinson, N. J. (2009) How do bacterial cells ensure that metalloproteins get the correct metal? *Nat. Rev. Microbiol. 7*, 25–35.
41. Mulrooney, S. B., and Hausinger, R. P. (2003) Nickel uptake and utilization by microorganisms. *FEMS Microbiol. Rev. 27*, 239–261.
42. Kuchar, J., and Hausinger, R. P. (2004) Biosynthesis of metal sites. *Chem. Rev. 104*, 509–525.
43. Soriano, A., Colpas, G. J., and Hausinger, R. P. (2000) UreE stimulation of GTP-dependent urease activation in the UreD-UreF-UreG-urease apoprotein complex. *Biochemistry 39*, 12435–12440.
44. Soriano, A., and Hausinger, R. P. (1999) GTP-dependent activation of urease apoprotein in complex with the UreD, UreF, and UreG accessory proteins. *Proc. Natl. Acad. Sci. U.S.A. 96*, 11140–11144.

45. Maier, T., Lottspeich, F., and Bock, A. (1995) GTP hydrolysis by HypB is essential for nickel insertion into hydrogenase of *Escherichia coli*. *Eur. J. Biochem. 230*, 133–138.
46. Leach, M. R., Sandal, S., Sun, H. W., and Zamble, D. B. (2005) Metal binding activity of the *Escherichia coli* hydrogenase maturation factor HypB. *Biochemistry 44*, 12229–12238.
47. Dias, A. V., Mulvihill, C. M., Leach, M. R., Pickering, I. J., George, G. N., and Zamble, D. B. (2008) Structural and biological analysis of the metal sites of *Escherichia coli* hydrogenase accessory protein HypB. *Biochemistry 47*, 11981–11991.
48. Rees, D. C. (2002) Great metalloclusters in enzymology. *Annu. Rev. Biochem. 71*, 221–246.
49. Zambelli, B., Danielli, A., Romagnoli, S., Neyroz, P., Ciurli, S., and Scarlato, V. (2008) High-affinity Ni^{2+} binding selectively promotes binding of *Helicobacter pylori* NikR to its target urease promoter. *J. Mol. Biol. 383*, 1129–1143.
50. Larkin, M. A., Blackshields, G., Brown, N. P., Chenna, R., McGettigan, P. A., McWilliam, H., Valentin, F., Wallace, I. M., Wilm, A., Lopez, R., Thompson, J. D., Gibson, T. J., and Higgins, D. G. (2007) ClustalW and ClustalX version 2. *Bioinformactics 23*, 2947–2948.